# Hough transform implementation to evaluate the morphological variability of the moon jellyfish (*Aurelia* sp.)

**Justine Gadreaud[1,*] · Céline Lacaux[2] · Agnès Desolneux[3] · Bertrand Martin-Garin[4] · Alain Thiéry[1]**

[1] Aix Marseille Univ, Univ Avignon, CNRS, IRD, IMBE, Marseille, France

[2] Avignon Université, LMA EA 2151, F-84000, Avignon, France

[3] CMLA (UMR CNRS 8536), ENS Paris-Saclay, Cachan, France

[4] Aix Marseille Univ, CNRS, IRD, Coll France, CEREGE, Aix-en-Provence, France

* Corresponding author: justine.gadreaud@imbe.fr +33 (0)663894175

## Abstract

Variations of the animal body plan morphology and morphometry can be used as prognostic tools of their habitat quality. The potential of the moon jellyfish (*Aurelia* spp.) as a new model organism has been poorly tested. However, as a tetramerous symmetry organism, it exhibits some variations in radial symmetry number. A pertinent list of morphological – number of gonads – and morphometric characteristics – e.g. ratio of the gonads area on the umbrella area – has been established to describe the morphology of 19 specimens through an image analysis. The method uses for the first time the Hough transform to approximate the gonads and the umbrella by ellipses and automatically extracts the morphometric data. The results highlight two discriminant parameters: distance between the center of the gonads and the center of the umbrella, and the individual variability of the gonad eccentricity, both higher in jellyfishes with 5 gonads. Additionally, the relative size of the gonads is not different between tetramerous and

non-tetramerous jellyfishes bringing some hypothesis about fitness advantages or disadvantages. Combined to ecotoxicological bioassays to better understand the causes of this developmental alteration, this optimizable method can become a powerful tool in the symmetry description of an *in situ* population.

**Keywords** Jellyfish · Morphometry · Symmetry disorder · Hough transform

## Introduction

*Jellyfish proliferations and asymmetric specimens of* Aurelia *spp.*

Over the last decades, the proliferation of adult jellyfishes has increased worldwide both in intensity and frequency along many marine coastal areas causing harmful societal inconveniences for industry and populations such as reduction of the fishery production, tourism, stinging of swimmers, etc. (Dong et al. 2010; Purcell et al. 2007; Richardson et al. 2009). It is commonly accepted that part of these blooms are a consequence of environmental changes often induced by intensive anthropogenic disturbance (Purcell 2005; Richardson et al. 2009) such as eutrophication, overfishing, translocation, habitat modification, etc. (Dong et al. 2010; Purcell 2005; Purcell et al. 2007; Richardson et al. 2009). The moon jellyfish *Aurelia* sp. is a diploblastic Semaeostomeae cnidarian with a worldwide distribution and the most common jellyfish in Europe coastal environments (Yuan et al. 2008). Scyphomedusae including moon jellyfish are tetramerous by definition with a stomach divided in four gastro-gonadic pouches by mesenteries in the center of their umbrella (Fig. **1**A). However, it can exhibit some variations in radial symmetry number (Brusca et al. 2016) (Fig. **1**B and C). The proportion of the non-tetramerous specimen in wild population has been estimated around 2 % and sparsely varies depending on the location (Gershwin 1999). The public aquariums also notice around 6–15 % of non-tetramerous jellyfishes in their populations (**Tab. 2**).

**Tab. 1** Rough estimations of non-tetramerous jellyfish proportions in public aquariums – personal observations.

| **Public aquariums** | Monterey Bay (USA) | Monaco | Barcelona (Spain) | La Rochelle (France) | Vancouver (Canada) |
|---|---|---|---|---|---|
| **Dates** | 10 August 2013 | 3 November 2014 | 1 June 2016 | 20 December 2016 | 13 August 2017 |
| **Non-tetramerous jellyfish proportions** | 11,5 % ($n$ = 122) | 6 % ($n$ = 160) | 15 % ($n \approx 80$) | 9 % ($n \approx 200$) | 13 % ($n$ = 120) |

In the Berre lagoon at 20 km west of Marseille (France), proliferation events of the moon jellyfish *Aurelia* sp. were observed in brackish environments as those of the summers 2006 and 2008 with a high proportion (≈ 6–7 %) of non-tetramerous specimens (Delpy et al. 2012) (**Fig. 7**). These phenotypic responses may be caused by a disturbance in the developmental process during the strobilation and the morphogenesis of the ephyrae. Indeed the Berre lagoon is the largest French lagoon of the Mediterranean coast: its environment is often affected by chemical pollutions and anthropogenic effluents (Accornero et al. 2008; Gadreaud et al. 2017; Rigaud et al. 2011).

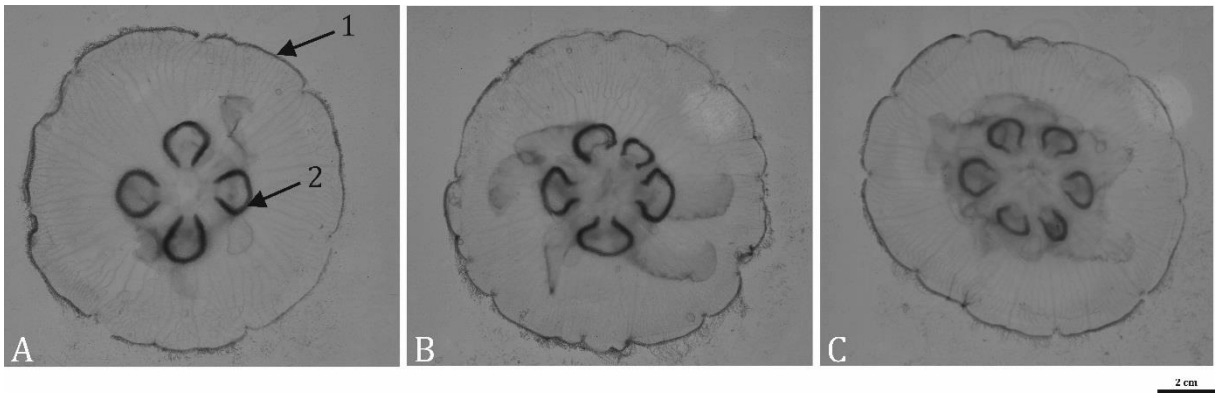


**Fig. 1.** Specimen of *Aurelia* sp. sampled in the Berre lagoon; 1: umbrella; 2: gastro-gonadic pouches (gonads); A) a tetramerous symmetry N = 4 gonads; B) and C) a non-tetramerous symmetry, N = 5, and N = 6 gonads respectively.

*Symmetry disorders as a biomarker*

The body symmetry (*Bauplan* concept *sensu* Brusca et al.) appeared early in the evolution process around ca. 575 million years ago (Ediacaran age) (Brusca et al. 2016). It can be defined

as a balanced distribution of duplicate body part. It is a common characteristic of the eumetazoans; all the animals excepting the sponges, but including the cnidarian phylum. As primitive organisms, each stage of cnidarian life cycle exhibits a vertical polar axis and a tetramerous radial symmetry axis from the center of the oral surface (Fig. **2**).

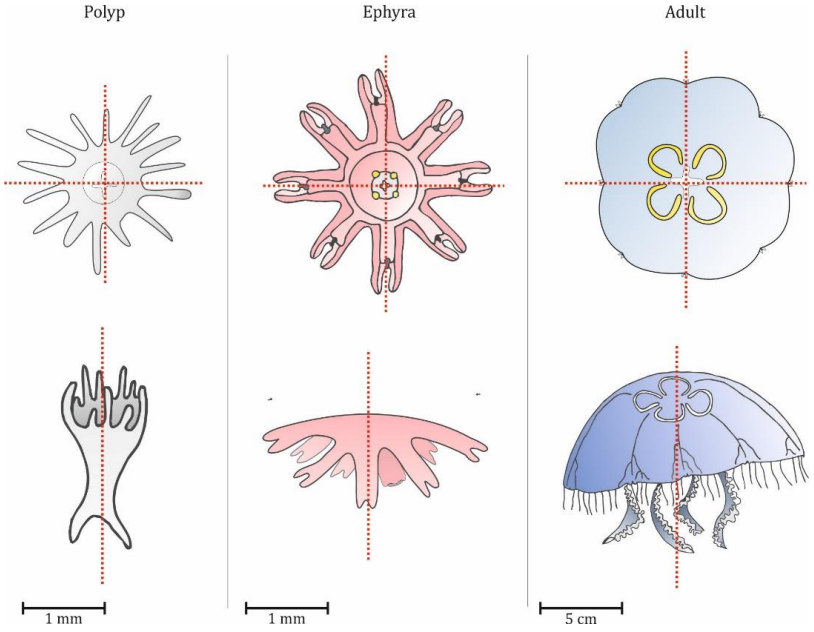


**Fig. 2.** Symmetry at each stage of the *Aurelia* spp. jellyfishes: tetramerous radial symmetry (oral face view) and vertical polar axis on polyp, ephyrae and medusae.

The characterization and the quantification of the elliptic characters of the jellyfish (global shape and number of gastro-gonadal pouches of the tetramerous and non-tetramerous specimens) remain a preliminary challenge to provide a database on the proportion of asymmetric jellyfishes and to evaluate the evolutionary advantages of reproduction or feeding. During a proliferation event of the moon jellyfish, the specimens can be easily sampled and photographed directly on the boat. Then, photography is a good tool to accumulate data in a short amount of time. It is also a good support to start morphologic and morphometric analysis using algorithms.

*Automatic morphometric analysis on images*

Algorithms for edge detections are particularly widely used in computational biology for characterization, quantification, or feature extractions. They aim at identifying points, lines or

outlines in an image. Classical edge detectors proceed to the extraction of images or mesh discontinuities. The result is a 2-bit image where black pixels correspond to the outline and white ones to the background. However, other algorithms are necessary for the objects displaying a simple geometry such as lines, circles, and ellipses, resulting to the common use of two feature extraction techniques: the fitting methods and the generalized Hough transform. The Hough Transform has been introduced by Hough for line detection but it allows also to detect parametric curves in an image, such as circles or ellipses (Ballard 1981; Hough 1962). Each edge point of the image votes for all curves passing through it: the method chooses the curves receiving the most votes. In practice, the space of possible parameters is discretized and the votes are stored in an *accumulator* array: the discretization influences the precision of the method (Duda and Hart 1972; Maitre 1985).

The objective of this present study is to develop an automatic image analysis method using for the first time the Hough transform on jellyfish to approximate the gonads and the umbrella by ellipses. The original step sheet includes: i) implementation of the detection of ellipses by Hough transform in Matlab® (R2017); ii) extraction of the main morphologic and morphometric characteristics of a control dataset of jellyfishes images; iii) statistical analysis on the morphometric parameters to highlight the discriminant ones between the tetramerous jellyfishes and the non-tetramerous ones.

## Materials and methods

*Samples, image acquisition and treatment*

The jellyfish image acquisition was performed with a Nikon® D800 camera coupled with a Nikkor 35 mm (AF 35 mm *f* / 10) lens, and resulted on a 36.3 Mo pixel photography for each specimen (Fig. **1**). A plastic blue background was placed underneath the jellyfish to enhance the contrast and have a better view on the organs – as the organism is transparent. The main

morphological characteristics of interest in this study are the ellipse shape parameters of the umbrella, the number of gastro-gonadic pouches (thenceforward simplified *gonads* throughout the text) and the ellipse shape parameters of each one of them (Fig. **1**). A Gaussian filter with standard deviation $\sigma = 20$ was applied in Matlab® (R2017) to each image. They were also resized keeping only $1/20^2$ pixels from the original: in the original image, $275 \times 275$ pixels correspond to 1 cm$^2$, in the reduced one, one pixel corresponds to $^4/_{55^2}$ cm$^2$.

*Algorithm details*

Since the gonads and the umbrella are not perfect ellipses and the gonads are often not even closed curves, those problems are non-trivial. The definition of an ellipse $\mathcal{E}$ involves five parameters: the center $C = (x_C, y_C)$, the orientation $\alpha \in [0, \pi]$, the semi-major axis $a$, the semi-minor axis $b$ (Fig. **3**). The eccentricity $e$ of the ellipse is given by the Equation (1).

$$e = \sqrt{\frac{1-b^2}{a^2}} \qquad (1)$$

For each jellyfish image, $\mathcal{E}_0$ denotes the ellipse corresponding to the umbrella; $\mathcal{E}_1, \ldots, \mathcal{E}_N$ the ellipses corresponding to the $N$ gonads (clockwise order) and $C_j$ denotes the center of each $\mathcal{E}_j$ (Fig. **3**).

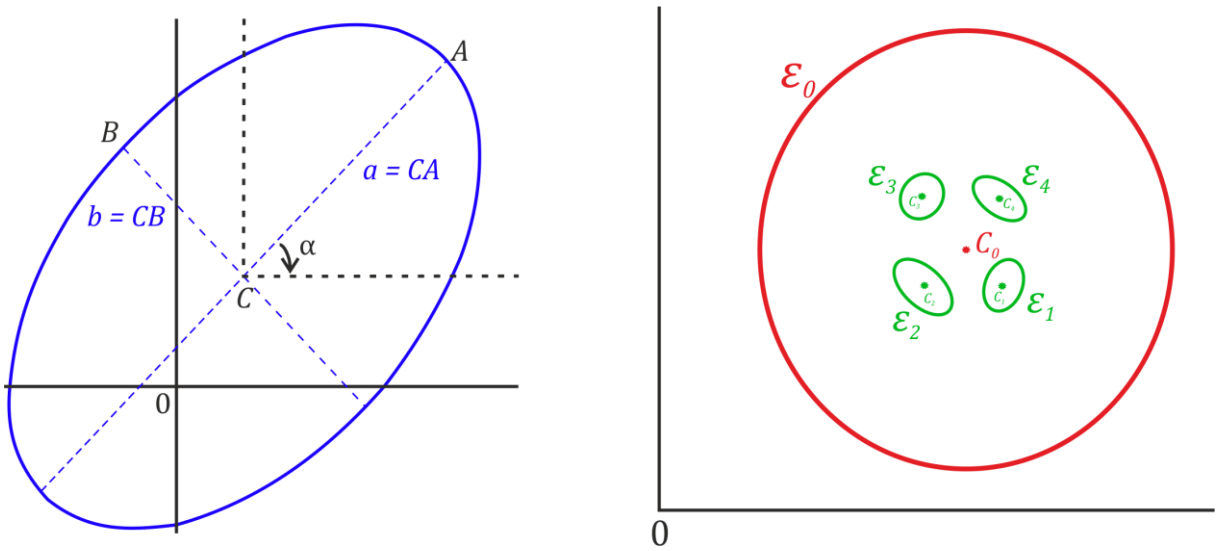


**Fig. 3.** On the left: ellipse $\mathcal{E}$ parameters; on the right: ellipses in a tetramerous jellyfish (with N = 4 gonads).

The implementation of the Hough transform proposed here is based on the parametrization of each ellipse by $C = (x_C, y_C)$, $\alpha$, $b$, and the eccentricity $e \in [0,1[$ (Equation (2)).

$$\begin{cases} x = x_C + \frac{b\cos(\theta-\alpha)}{\sqrt{1-e^2\cos^2(\theta-\alpha)}} \\ y = y_C + \frac{b\sin(\theta-\alpha)}{\sqrt{1-e^2\cos^2(\theta-\alpha)}} \end{cases} \quad (2)$$

where $\theta$ describes $[0, 2\pi]$. The major semi-axis is then equal to $\frac{b}{\sqrt{1-e^2}}$.

The Hough transform retrieves the parameter $(x_C, y_C, \alpha, e, b)$ corresponding to the ellipses in the image, using a 5-dimensional discrete accumulator array. But the range of possible parameters is huge and depends on the size of the image; the method can be very slow. To reduce the computational time, the advantage of some *a priori* on the parameters values has been taken. First the approximate centers of the umbrella and gonads ellipses are set by the user: the detection will focus only on possible centers around these initialized positions, which reduces drastically the possible sets of centers $C = (x_C, y_C)$. The size of the neighborhood is a parameter chosen in function of the image size. An *a priori* of the range for the semi-parameters $b$ has been taken; this can be done for each ellipse if needed. The eccentricity is bounded by a value $e_{max} < 1$ to avoid too flat ellipses and false detections.

The thresholds of the Canny edge detector are automatically chosen by Matlab® (R2017) with the toolbox *Image Processing Toolbox*. For each image, the mesh size for the orientation $\alpha$ is $0.2$, the mesh size for the eccentricity $e$ is $0.05$ and $e$ varies between $0$ and $0.85$, the range for the semi-minor axis of the umbrella is $[50{:}\,150]$ (expressed in pixels). For the detection of the gonads, [1:10] has been used as range for the semi-minor axis $b$. On few images, this range was changed for some specific gonads due to their small size: the peaks in accumulator array that should characterize them is not so evident when choosing a comparatively large range for parameter $b$.

The implemented algorithm provides each ellipse parameters $\left(x_{C_j}, y_{C_j}, \alpha_j, e_j, b_j\right)$ for $j = 0 \ldots N$. Then, the following quantities are provided: the area $\mathcal{A}_j$ of $\mathcal{E}_j$ (in cm$^2$, Equation (3)); the ratio $\wp_j$ (Equation (4)); the distances $C_0C_j$ (in cm) between the center of the gonads and the umbrella center.

$$\mathcal{A}_j = \pi a_j b_j = \frac{\pi b_j^2}{\sqrt{1-e_j^2}} \qquad (3)$$

$$\wp_j = \frac{\mathcal{A}_j}{\mathcal{A}_0} \qquad (4)$$

# Results

*Dataset*

To test the algorithm, the dataset is composed of 19 jellyfishes sampled during two proliferations (September of 2008 and March 2006) at the same location (Berre Lagoon, south of France). They are divided in 4 groups depending on their number of gonads (Tab. **2**). The morphologic and morphometric parameters from the jellyfishes having 3 and 6 gonads were not included in the statistical analysis because of their very low workforce ($n$ = 1 for both of these groups). Only the significant discriminant morphometric parameters highlighting difference between the tetramerous and non-tetramerous jellyfish groups, or giving pertinent morphological clues are exposed in these results.

**Tab. 2** Morphology details of the jellyfishes of the data basis

| | **Tetramerous jellyfishes** | **Non-tetramerous jellyfishes** | | | **Total** |
|---|---|---|---|---|---|
| **Number of gonads** | $N = 4$ | $N = 3$ | $N = 5$ | $N = 6$ | |
| **Number of jellyfishes** | n = 12 | n = 1 | n = 5 | n = 1 | 19 |

*3.2 Graphic results*

Fig. **4** shows the main morphologic features estimated by the algorithm: the ellipse detected for the umbrella and its center, the ellipses detected for each gonad and their center.

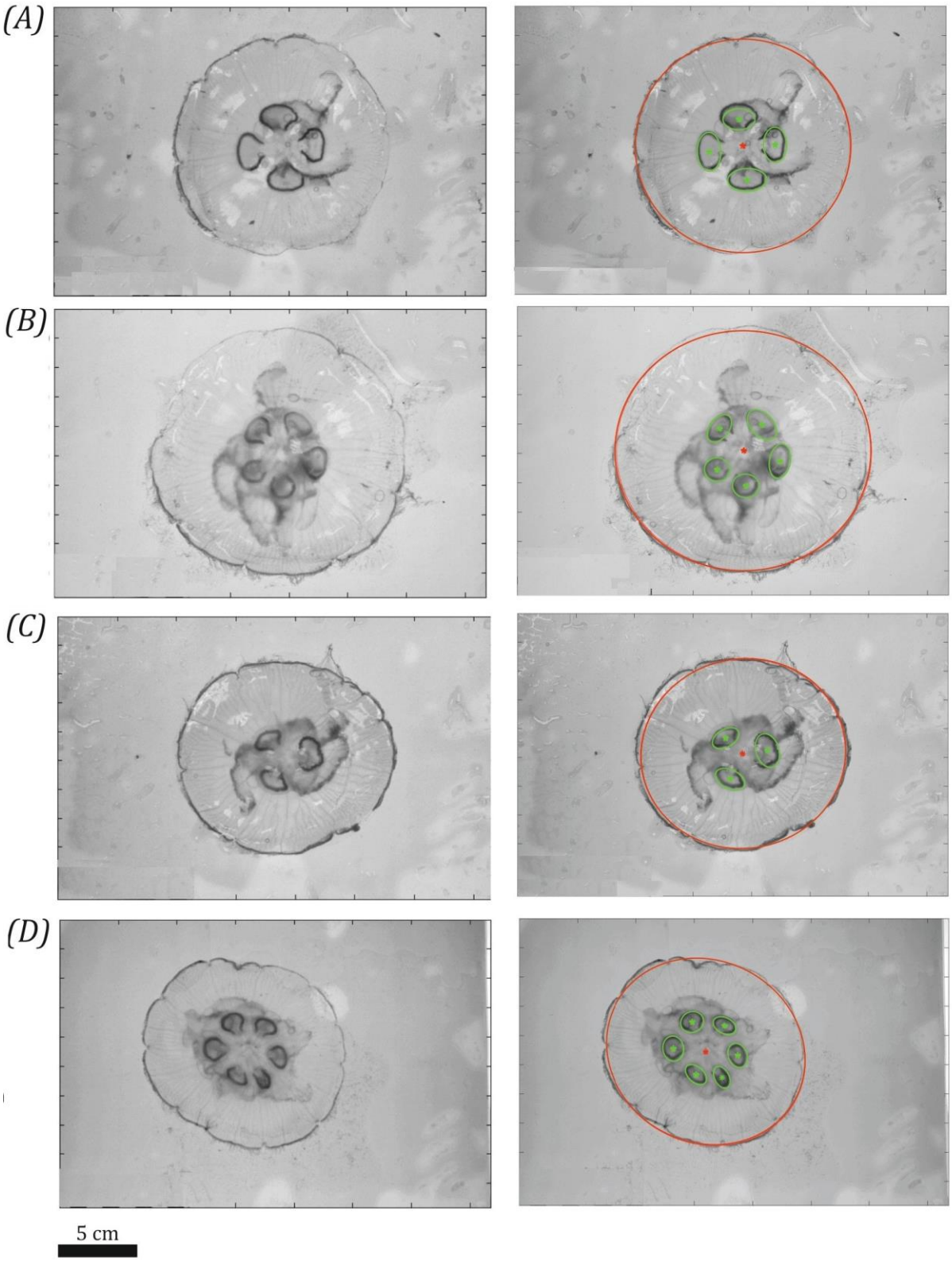


**Fig. 4.** Jellyfishes with 4 gonads (A), 5 gonads (B), 3 gonads (C) and 6 gonads (D). Left: grayscale image; right: grayscale image with detected ellipse: red for the umbrella and its center and green for the ellipses detected for each of the *N* gonads.

### *3.3. Ratio gonad area on area of the umbrella*

We wonder if for tetramerous and non-tetramerous jellyfishes, the relative size of the gonads is the same. To obtain a criterion of comparison which does not depend on the organism size, we propose to study the ratio $\wp$ (Equation (5)).

$$\wp = \frac{area\ of\ one\ gonad}{area\ \mathcal{A}_0\ of\ the\ umbrella} \times 100\ (\%) \qquad (5)$$

For each jellyfish $i = 1,..n$ with $N$ gonads, $N$ observations $\wp_{i1}, \dots, \wp_{iN}$ of the ratio $\wp$ have been evaluated (Fig. **5**). From the biological point of view, the gonads are not differentiable and in particular, grouping the observations using the numbering proposed by the algorithm does not make sense. Because of this, we consider that for each fixed $N$, these data form one sample, so that we have one sample of size $n_1 = 48$ corresponding to jellyfishes with $N = 4$ gonads and one sample of size $n_2 = 25$ corresponding to jellyfishes with $N = 5$ gonads. This assumption is reinforced by applying to each group of jellyfishes ($N = 4$ and $N = 5$ gonads) a bilateral runs test for randomness using the median as a separator (p-value = 0.6599 for the tetramerous jellyfishes group and p-value = 1 for the non-tetramerous ones). Then the bilateral Mann & Whitney test concludes that the medians of $\wp$ for the two groups ($N = 4$, and $= 5$ ) are not significantly different (p-value = 0.565).

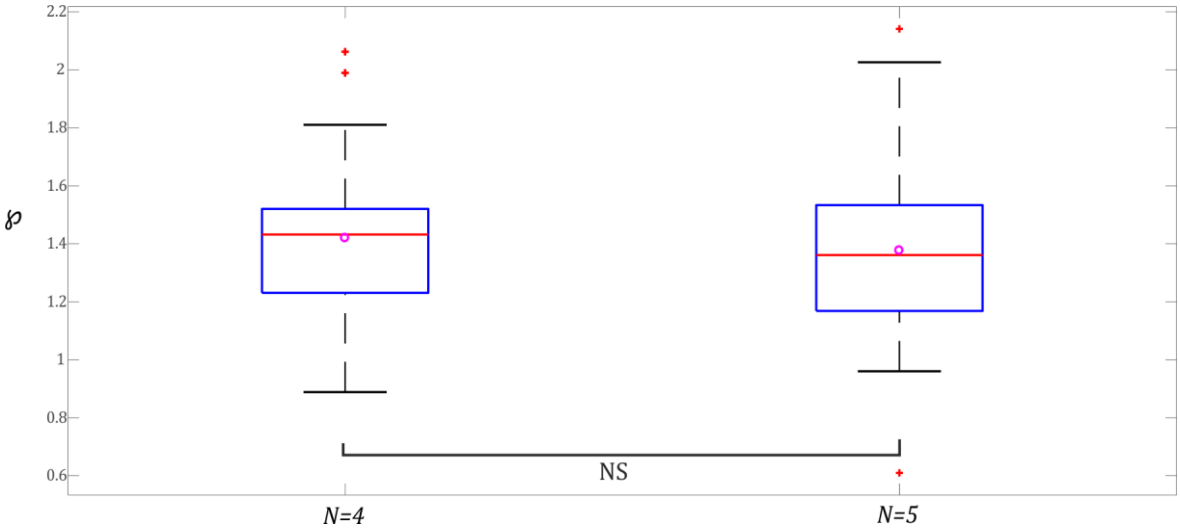


**Fig. 5.** Boxplot of the ratios $\wp$ for tetramerous jellyfish group ($N = 4$ gonads; $n_1 = 48$ data) and non-tetramerous jellyfish group ($N = 5$ gonads; $n_2 = 25$ data); *NS*: p-value > 0.05 (Mann & Whitney comparison test).

*Distance of gonad center to umbrella center*

We wonder if for tetramerous and non-tetramerous jellyfishes, the gonads are located at the same distance from the umbrella center. To take into account the size of the jellyfish and its anisotropy (that is its elliptic shape), we characterize the distance between a gonad and the umbrella center by the ratio $D$ (Equation (6)) where $C_0$ is the umbrella center and $C$ the gonad center.

$$D = \frac{area\ of\ a\ circle\ with\ radius\ C_0C}{area\ \mathcal{A}_0\ of\ the\ umbrella} \times 100\ (\%) \qquad (6)$$

This ratio is then independent of the jellyfish size and the smaller it is the closer to the umbrella center the gonad is.

As in the previous study, for each jellyfish $i = 1 \ldots n$ with $N$ gonads, $N$ values $D_{11}, \ldots, D_{iN}$ of the ratio $D$ have been evaluated. For each fixed $N$, as previously we assume that the collected data form one sample and apply as verification a bilateral runs test for randomness using the median as a separator: p-value = 0.8866 for the tetramerous jellyfishes group and p-value = 0.1398 for the non-tetramerous ones. For the non-tetramerous group, the p-value is small but this may be due to the small size of the tested sample. With this in mind, we continue the study by applying a unilateral Mann & Whitney test which concludes that the median of $D$ is lower

for the tetramerous jellyfishes than for the non-tetramerous ones (p-value = 0.0454, Fig. **6**). In other words, this study suggests that for $N = 5$ gonads, the gonads of the jellyfishes are located further from the umbrella center than in tetramerous jellyfishes.

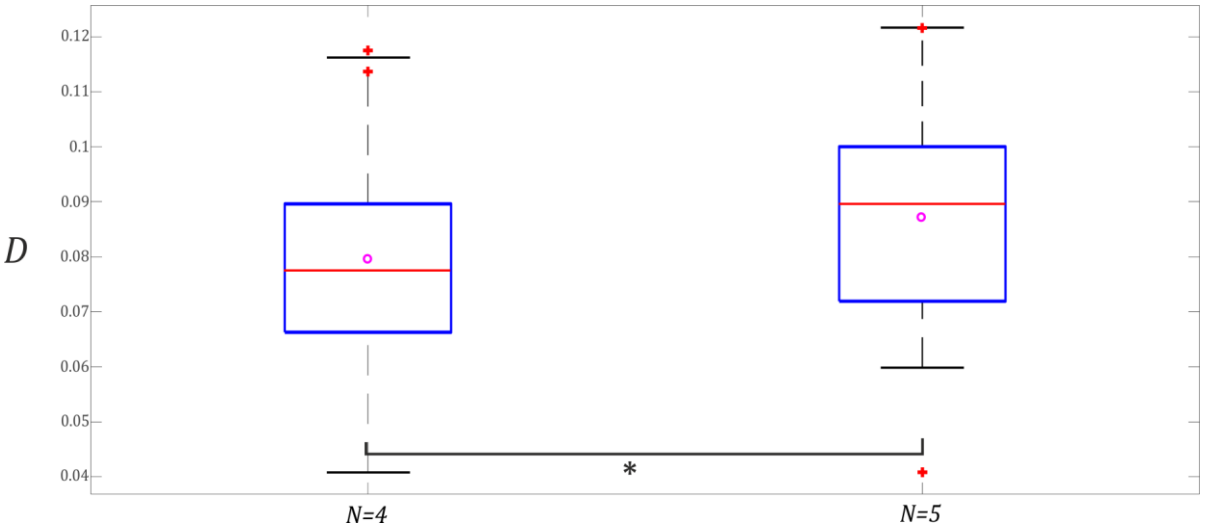


**Fig. 6.** Boxplot of the ratios D for tetramerous jellyfishes' group ($N = 4$ gonads; $n_1 = 48$ data) and non-tetramerous jellyfishes group ($N = 5$ gonads; $n_2 = 25$ data).

*The gonads eccentricity*

This part compares the gonad eccentricity between tetramerous and non-tetramerous jellyfishes.

We first studied the individual mean eccentricity $\bar{e}$ (Equation (7))

$$\bar{e} = \frac{1}{N}\sum_{j=1}^{N} e_j \qquad (7)$$

It is the mean of the gonads eccentricity of one jellyfish: we have one observation of $\bar{e}$ for each jellyfish, leading to one sample of size $n_1 = 12$ for the group with $N = 4$ gonads and one sample of size $n_2 = 5$ for the group with $N = 5$ gonads. The bilateral Mann & Whitney test concludes that there is no significant difference between those two groups as regards the individual mean eccentricity $\bar{e}$.

As working on the individual mean eccentricity, our interest grew on the individual variability of the gonad's eccentricity: we decided to focus on $S^2$ (Equation (8))

$$S^2 = \frac{1}{N-1}\sum_{j=1}^{N}(e_j - \bar{e})^2 \qquad (8)$$

A unilateral Mann & Whitney test has been performed to compare the individual variability $S^2$ of tetramerous jellyfishes ($n_1 = 12$ data) and of jellyfishes with $N = 5$ gonads ($n_2 = 5$ data). Keeping in mind the small sizes of the samples, this test concludes that there is a significant difference for the median of $S^2$ between the two groups (p-value = 0.0381): the jellyfishes with $N = 5$ gonads exhibit a higher gonad eccentricity variability than the tetramerous ones.

## Discussion

*Implementation of Hough transform in biology*

As conspicuous and important component of the ecosystem, medusae have received growing interest over the last decades as numerous proliferations have been reported with increasing frequencies in all seas and oceans. This present study proposes an optimizable tool to quantify and characterize the main *Aurelia* spp. morphometric characteristics through aerial images of *in situ* organisms during a proliferation. Ellipse detection algorithms have been already implemented to characterize circular biological objects such as cells in microbiology microscopic images (Cai et al. 2011; Kumagai and Hotta 2012; Lehmussola et al. 2005). Here in this paper, it is the first time that the Hough transform has been used to extract morphometric characteristics on jellyfishes highlighting new challenge for the implementation such as to detect small ellipses (gonads) in a bigger one (umbrella) and to characterize them as *N* samples of one individual. The algorithms used on cells images have limits in their application, mainly when there is a superposition of ellipses (agglomerated cells) or two ellipses connected (budding cells) (Denimal et al. 2017). This forced the biologist to manually set some parameters for a group of images preventing its automation just as here, where the images have to be separated in classes and few parameters fixed to limit the computational time but preventing a full automation. Recently, few authors proposed new solutions such as using gradient accumulation matrix (Denimal et al. 2017) or color variation detections by a computer vision

system to improve the automation potential (Murillo-Bracamontes et al. 2012). Those solutions are currently investigated for an application on aerial jellyfish proliferation captured by drone as shown on Fig. **7**.

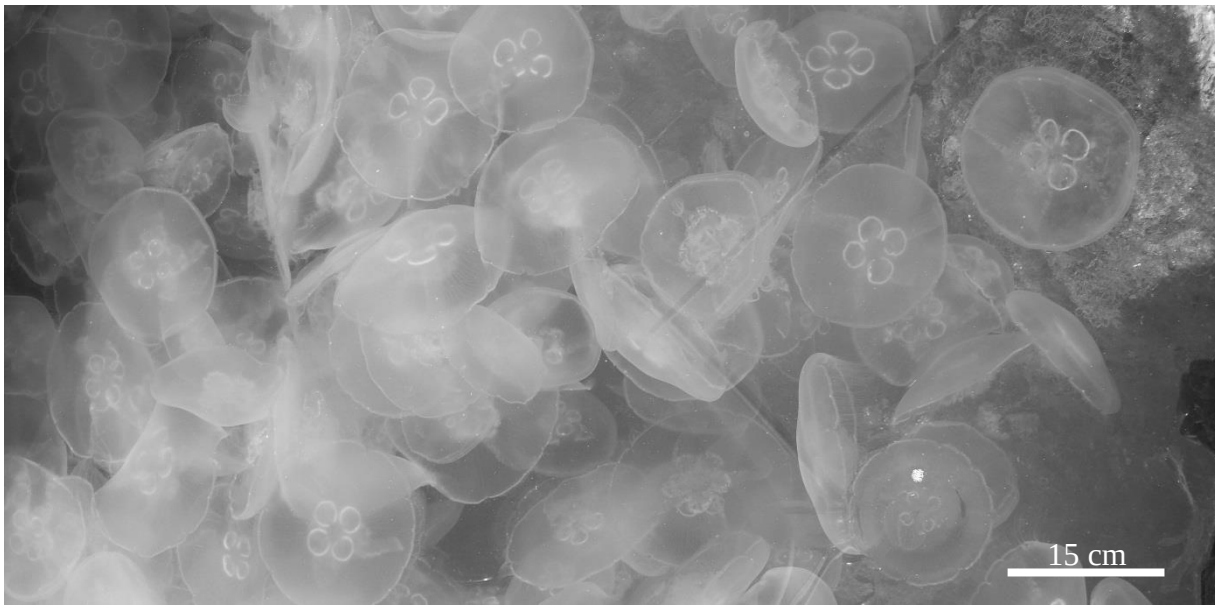


**Fig. 7.** Aerial image of a proliferation of the moon jellyfish *Aurelia* sp. in the Berre lagoon (Southern France) in July 2008 Alain Thiéry©

*Discriminant morphometric characteristics*

Even if the algorithm is optimizable and the sample small, the analysis of the morphometric data permitted to highlight the remarkable characteristics of the tetramerous jellyfishes and the non-tetramerous ones (Fig. **8**). The ratio $\wp$ rendering the size of the gonads brings out no significant difference between the two groups. The individual variability of the gonads eccentricity $S^2$ (higher for the jellyfishes with 5 gonads) and the ratio $D$ rendering the distance of gonad center to umbrella center – higher for the jellyfishes with 5 gonads – are discriminant to distinguish the jellyfishes with 4 gonads and the jellyfishes with 5 gonads.

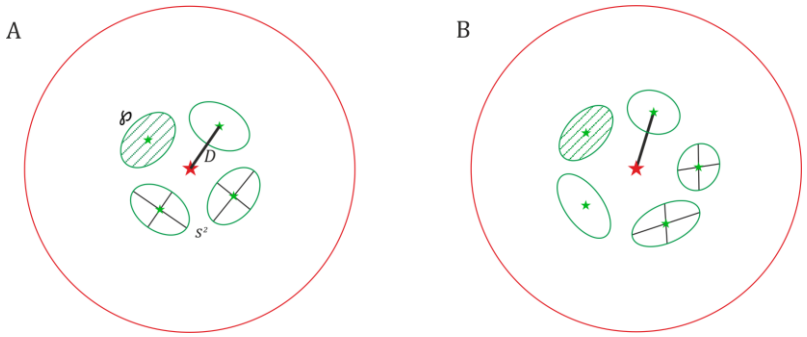


**Fig. 8.** Conceptual scheme of the 3 different morphometric characteristics remarkable between the A: tetramerous jellyfishes and B: the non-tetramerous jellyfishes. ℘ ratio rendering the relative size of the gonads; $S^2$ the individual variability of the gonad's eccentricity; D ratio rendering the relative distance of the gonad center to the umbrella center.

By a hypothetical extrapolation, the other non-tetramerous symmetry case (*i.e.* 3 gonads and 6 gonads) are relatable too: if the general body plan is respected, there is no isometry number-of-gonads dependent. In the perspective of analyzing numerous aerial images of jellyfishes during a proliferation, those three parameters would allow a good description of the population in terms of proportion of non-tetramerous individuals. The force of these analysis is that the results are not population-dependent and organism size-dependent allowing a large application. This optimizable tool is opening a new field of research: the challenge is now to understand what can cause high rate of non-tetramerous individual in a population. As started by Gadreaud et al. (2017), new ecotoxicological bioassays have to be conducted to better understand the causes of this developmental perturbations but also understand the physiological consequences of those morphologies.

*Perspective: physiology studies*

Because the relative size of the gonads is the same in non-tetramerous jellyfishes than the tetramerous one (Fig. **5**), the mobility of those dissymmetric jellyfishes with more gonads may be affected because the proportion of the muscle in the umbrella is reduced – more surface occupied by the gonads. It may also modify the physiology and the resource allocation: as a reproduction organ, the gonad is a high consumer of energy. Associated with each gonad comes a gastric pouch increasing the potential digestion capacity. More than the number of gonads,

the alteration of the tetramerous symmetry also includes the number of *rhopalia* (sensor cells) and sometimes the number of tentacles. Because this dissymmetry appears at a clonal level – for one polyp, normal and dissymmetric *ephyrae* can be produced – the hereditary of these abnormalities is not obvious (Gershwin 1999). In 1999, Gershwin collected a large amount of data through sample analysis and bibliographic reports from 1700s to 1990s. She submitted the hypothesis that the proportion of abnormal development in *Aurelia* spp. can be related to stress, environmental variations, but mainly pollution exposition (Gershwin 1999). This last point was confirmed by the study of Gadreaud *et al.* (2017) in 2017 relating higher proportion of non-tetramerous *ephyrae* born from polyps exposed to emergent xenobiotics, and proposing then this organism as a new model in nanoecotoxicology. Bioassays are currently in progress to test those last results: *Aurelia* sp. polyps are exposed to silver and titanium dioxide nanoparticles which are emergent xenobiotics in marine environment (Gadreaud et al. 2017).

**Acknowledgments**

The authors acknowledge financial support from the French ANSES (Agence nationale de sécurité sanitaire de l'alimentation, de l'environnement et du travail – 'DecoNano' program) and the French Ministry of Higher Education and Scientific Research. They also thanks the GIPREB (syndicat intercommunal pour la sauvegarde de l'étang de Berre).

## Code details

**Algorithm 1** Detection of the umbrella and the gonads

**Inputs**:
$I \leftarrow$ original image
$N \leftarrow$ number of gonads
$db \leftarrow$ mesh size for the semi minor axis
$de \leftarrow$ mesh size for the eccentricity
$\delta \leftarrow$ precision parameter

**Step 1. Pre processing**
Convert $I$ to a greyscale image
Apply a Gaussian filter (to denoise the image), with fixed variance
Down sample the image (to reduce the number of pixels)
Apply the Canny Ege detector:
    $E \leftarrow$ binary edge image ▷ Use the default parameters of Matlab.
**Step 2. Ellipses detection**
**for** $j = 0$ to $N$
    $b \leftarrow [b_{min} : \mathrm{d}b : b_{max}]$
    $(x_{0C}, y_{0C}) \leftarrow$ approximative center of the ellipse $\mathcal{E}_j$
    Initialize accumulator array:
        $H \leftarrow 0$
    **for** $x_C = x_{0C} - \delta : x_{0C} + \delta$
        **for** $y_C = y_{0C} - \delta : y_{0C} + \delta$
            **for** $\alpha = 0 : \mathrm{d}\alpha : \pi$
                **for** $e = 0 : \mathrm{d}e : e_{max}$
                    **for** $(x, y)$
                        **if** $E(x, y) == 1$
                        Compute $b$ such that $(x, y) \in \mathcal{E}(x_C, y_C, \alpha, e, b)$
                        Increase the counter cell of $H$ corresponding to $(x_C, y_C, \alpha, e, b)$
                        **end if**
                    **end for**
                **end for**
            **end for**
        **end for**
    **end for**
    Keep the parameters $(x_C, y_C, \alpha, e, b)$ maximizing the counter $H$
**end for**

## References


Accornero A, Gnerre R, Manfra L (2008) Sediment concentrations of trace metals in the Berre Lagoon (France): an assessment of contamination. Archives of Environmental Contamination and Toxicology 54:372–385 doi:10.1007/s00244-007-9049-6

Ballard DH (1981) Generalizing the Hough transform to detect arbitrary shapes. Pattern Recognition 13:111–122 doi:https://doi.org/10.1016/0031-3203(81)90009-1

Brusca RC, Moore W, Shuster SM (2016) Invertebrates vol 3rd Edition. Sinauer Assoc. Inc. , USA

Cai Z, Chattopadhyay N, Liu WJ, Chan C, Pignol J-P, Reilly RM (2011) Optimized digital counting colonies of clonogenic assays using ImageJ software and customized macros: comparison with manual counting. International Journal of Radiation Biology 87:1135–1146 doi:10.3109/09553002.2011.622033

Delpy F, Pagano M, Blanchot J, Carlotti F, Thibault-Botha D (2012) Man-induced hydrological changes, metazooplankton communities and invasive species in the Berre Lagoon (Mediterranean Sea, France). Marine Pollution Bulletin 64:1921–1932 doi:http://dx.doi.org/10.1016/j.marpolbul.2012.06.020

Denimal E, Marin A, Guyot S, Journaux L, Molin P (2017) Automatic biological cell counting using a modified gradient Hough transform. Microscopy and Microanalysis 23:11–21 doi:10.1017/S1431927616012617

Dong Z, Liu D, Keesing JK (2010) Jellyfish blooms in China: dominant species, causes and consequences. Marine Pollution Bulletin 60:954–963 doi:http://dx.doi.org/10.1016/j.marpolbul.2010.04.022

Duda RO, Hart PE (1972) Use of the Hough transformation to detect lines and curves in pictures. Journal of the Association for Computing Marchinery 15:11–15

Gadreaud J, Martin-Garin B, Artells E, Levard C, Auffan M, Barkate A-L, Thiéry A (2017) The moon jellyfish as a new bioindicator: impact of silver nanoparticles on the morphogenesis. In: Mariottini GL (ed) Jellyfish: Ecology, Distribution Patterns and Human Interactions. Nova Science Publishers, Inc., pp 277–292

Gershwin L-A (1999) Clonal and population variation in jellyfish symmetry. Journal of the Marine Biological Association of the United Kingdom 79:993–1000

Hough PVC (1962) Method and means for recognizing complex patterns. United States Patent 3

Kumagai S, Hotta K Counting and radius estimation of lipid droplet in intracellular images. In: 2012 IEEE International Conference on Systems, Man, and Cybernetics (SMC), 14-17 Oct. 2012 2012. pp 67–71. doi:10.1109/ICSMC.2012.6377678

Lehmussola A, Selinummi J, Ruusuvuori P, Niemisto A, Yli-Harja O (2005) Simulating fluorescent microscope images of cell populations. Conf Proc IEEE Eng Med Biol Soc 3:3153–3156 doi:10.1109/iembs.2005.1617144

Maitre H (1985) Un panorama de la transformation de Hough. Traitement du Signal 2:305–317

Murillo-Bracamontes EA, Martinez-Rosas ME, Miranda-Velasco MM, Martinez-Reyes HL, Martinez-Sandoval JR, Cervantes-de-Avila H (2012) Implementation of Hough transform for fruit image segmentation. Procedia Engineering 35:230–239 doi:https://doi.org/10.1016/j.proeng.2012.04.185

Purcell JE (2005) Climate effects on formation of jellyfish and ctenophore blooms: a review. Journal of the Marine Biological Association of the United Kingdom 85:461–476 doi:10.1017/S0025315405011409

Purcell JE, Uye S, Lo W (2007) Anthropogenic causes of jellyfish blooms and their direct consequences for humans: a review. Marine Ecology Progress Series 350:153–174

Richardson AJ, Bakun A, Hays GC, Gibbons MJ (2009) The jellyfish joyride: causes, consequences and management responses to a more gelatinous future. Trends Ecol Evol 24:312–322 doi:http://dx.doi.org/10.1016/j.tree.2009.01.010

Rigaud S, Radakovitch O, Nerini D, Picon P, Garnier JM (2011) Reconstructing historical trends of Berre lagoon contamination from surface sediment datasets: Influences of industrial regulations and anthropogenic silt inputs. Journal of Environmental Management 92:2201–2210 doi:http://dx.doi.org/10.1016/j.jenvman.2011.04.002

Yuan D, Nakanishi N, Jacobs D, Hartenstein V (2008) Embryonic development and metamorphosis of the scyphozoan *Aurelia*. Development Genes and Evolution 218:525–539 doi:10.1007/s00427-008-0254-8